Spectrochimica Acta Part A 85 (2012) 145–154

Contents lists available at SciVerse ScienceDirect

Spectrochimica Acta Part A: Molecular and Biomolecular Spectroscopy

journal homepage: www.elsevier.com/locate/saa

NMR, UV, FT-IR, FT-Raman spectra and molecular structure (monomeric and dimeric structures) investigation of nicotinic acid *N*-oxide: A combined experimental and theoretical study

Ahmet Atac[a,*], Mehmet Karabacak[b], Caglar Karaca[a], Etem Kose[a]

[a] Department of Physics, Celal Bayar University, Manisa, Turkey
[b] Department of Physics, Afyon Kocatepe University, Afyonkarahisar, Turkey

ARTICLE INFO

Article history:
Received 30 July 2011
Received in revised form
15 September 2011
Accepted 22 September 2011

Keywords:
Nicotinic acid *N*-oxide
DFT
NMR, UV, FT-IR and FT-Raman
HOMO–LUMO

ABSTRACT

In this work, the experimental and theoretical UV, NMR, and vibrational features of nicotinic acid *N*-oxide (abbreviated as NANO, $C_6H_5NO_3$) were studied. The ultraviolet (UV) absorption spectrum of studied compound that dissolved in water was examined in the range of 200–800 nm. FT-IR and FT-Raman spectra in solid state were observed in the region 4000–400 cm^{-1} and 3500–50 cm^{-1}, respectively. The ^1H and ^{13}C NMR spectra in DMSO were recorded. The geometrical parameters, energies and the spectroscopic properties of NANO were obtained for all four conformers from density functional theory (DFT) B3LYP/6-311++G(d,p) basis set calculations. There are four conformers, C_n, $n = 1–4$ for this molecule. The computational results identified the most stable conformer of title molecule as the C1 form. The complete assignments were performed on the basis of the total energy distribution (TED) of the vibrational modes, calculated with scaled quantum mechanics (SQM) method. ^{13}C and ^1H nuclear magnetic resonance (NMR) chemical shifts of the molecule were calculated by using the gauge-invariant atomic orbital (GIAO) method. The electronic properties, such as excitation energies, absorption wavelengths, HOMO and LUMO energies, were performed by CIS approach. Finally the calculation results were applied to simulate infrared, Raman, and UV spectra of the title compound which show good agreement with observed spectra.

1. Introduction

Nicotinic acid, NA (known as niacin, pyridine-3-carboxylic acid), belongs to the hydrophilic vitamin B complex. NA is a component of nicotinamide adenine dinucleotide (NAD) [1]. It is the foundation for a plethora of commercial compounds, from antibacterial and cancer drugs in the biomedical industry, in production of cosmetics, to pesticides and herbicides in the agrochemical industry, to charge control agents in photocopier toners [2]. NA has many important functions in animal and human feed. The different complexes metals of nicotinic [3], isonicotinic [4] and picolinic acids [5] were thoroughly investigated by different methods. Metal halide complexes of isonicotinic acid were synthesized and investigated with vibrational spectroscopy [6–8]. Karabacak et al. [9,10] investigated the molecular structure and vibration frequencies of 2-chloronicotinic acid and 6-chloronicotinic acid molecules with FT-IR and FT-Raman spectroscopy and quantum chemical calculations.

Pyridine *N*-oxides have applications in a wide range of fields including, for instance, industry, medicine, biochemistry and nanotechnology [11–16]. Structural and spectroscopic information has recently been reported for compounds with transition metals and lanthanides [15–19]. Pyridine carboxylic acid *N*-oxides have an oxygen atom in place of the nitrogen donor site but studies on ligand behavior toward lanthanides are limited [20], as so far only one dimeric lanthanum complex of 6-methyl picotinic acid *N*-oxide has been structurally determined [21].

DFT calculations are reported to provide excellent vibrational frequencies of organic compounds if the calculated frequencies are scaled to compensate for the approximate treatment of electron correlation, for basis set deficiencies and for the anharmonicity [21–25]. Experimental and theoretical vibrational spectra of nicotinic, picolonic and isonicotinic acids were studied by DFT calculations with different methods [26,27]. In addition Li-Ran and Yan [28] carried out experimental (UV and Raman) and theoretical (DFT) study of pyridine carboxylic acid (isonicotinic acid) in aqueous solution. Sala et al. [29] investigated vibrational modes of nicotinic acid by both experimental as well as theoretical

* Corresponding author. Tel.: +90 236 241 2151.
E-mail addresses: atacahmet2007@gmail.com, ahmet.atac@bayar.edu.tr (A. Atac).

1386-1425/$ – see front matter © 2011 Elsevier B.V. All rights reserved.
doi:10.1016/j.saa.2011.09.048

methods. However, literature survey reveals that to the best of our knowledge, no experimental and computational (DFT) spectroscopic study performed on the conformation, vibrational, NMR, UV and Raman spectra of free NANO. An extensive experimental spectroscopic study NANO was undertaken by recording their UV, NMR, FT-IR and FT-RAMAN spectra. We have carried out DFT calculations with the combined Becke's three-parameter exchange functional in combination with the Lee, Yang and Parr correlation functional (B3LYP). Theoretical investigations can facilitate the solution to the problems confronted in the experimental and computational techniques.

Carboxyl group in NANO is of four different positions, so that chosen four conformers of the title molecule were optimized to find energies at B3LYP/6-311++G(d,p) level of calculations. C1 form is the more stable conformer than the other conformers. The results of the theoretical and spectroscopic studies are reported herein. Also, the vibrational wavenumbers of C1 monomer and dimer conformers of NANO have also been calculated. Vibrational assignments were made based on total energy distribution (TED). Moreover, the gauge-including atomic orbital (GIAO) ^{13}C and ^{1}H chemical shifts calculations were done. The electronic properties, such as excitation energies, wavelengths and HOMO and LUMO energies, were performed by CIS approach.

2. Experimental

The compound NANO in solid state was purchased from Across Organics Company with a stated purity of 99% and it was used as such without further purification. The infrared spectrum of compound was recorded between 4000–400 cm^{-1} on a Perkin-Elmer FT-IR System Spectrum BX spectrometer which was calibrated using polystyrene bands and under 400 cm^{-1} on Bruker IFS 66/S. The sample was prepared using a KBr disc technique. The FT-Raman spectrum of compounds was recorded between 3500–50 cm^{-1} on FRA 106/S spectrometer. The ultraviolet absorption spectrum of NANO, solved in water, was examined in the range 200–800 nm using Shimadzu UV-1700 PC, UV–vis recording Spectrophotometer. NMR experiments were performed in Varian Infinity Plus spectrometer at 300 K. The compound was dissolved in DMSO. Chemical shifts were reported in ppm relative to tetramethylsilane (TMS) for ^{1}H and ^{13}C NMR spectra. NMR spectra were obtained at a base frequency of 75 MHz for ^{13}C and 400 MHz for ^{1}H nuclei.

3. Computational details

In this study, all the calculations were performed using Gaussian 09 [30]. The hybrid B3LYP [31,32] method based on Becke's three parameter functional of DFT and 6-311++G(d,p) basis set level were chosen and four possible conformers (C1, C2, C3 and C4) proposed than optimized for NANO. The optimized structural parameters were used in the vibrational frequencies, isotropic chemical shifts and absorption wavelengths. The vibrational frequencies, Infrared and Raman intensities for the planar (C_s symmetry group) structure of the molecule were calculated. We investigated all conformers with C_s symmetry group. The C1 and C2 isomers have no imaginary frequencies; however the C3 and C4 conformers had imaginary frequencies. We converted to non-planar (C_1 symmetry group) structure in case given no error for frequency values. Thus the stability of the optimized geometries is confirmed by frequency calculations, which gives positive values for all the obtained frequencies. Computed harmonic frequencies were scaled in order to improve the agreement with the experimental results. The vibrational wavenumbers for the four conformers are calculated with this method and then wavenumbers in the ranges from 4000 to 1700 cm^{-1} and lower than 1700 cm^{-1} are scaled with 0.958 and 0.983, respectively. [33]. The total energy distribution (TED) was calculated by using the scaled quantum mechanics SQM method and PQS program [34,35] in order to characterize of fundamental vibrational modes.

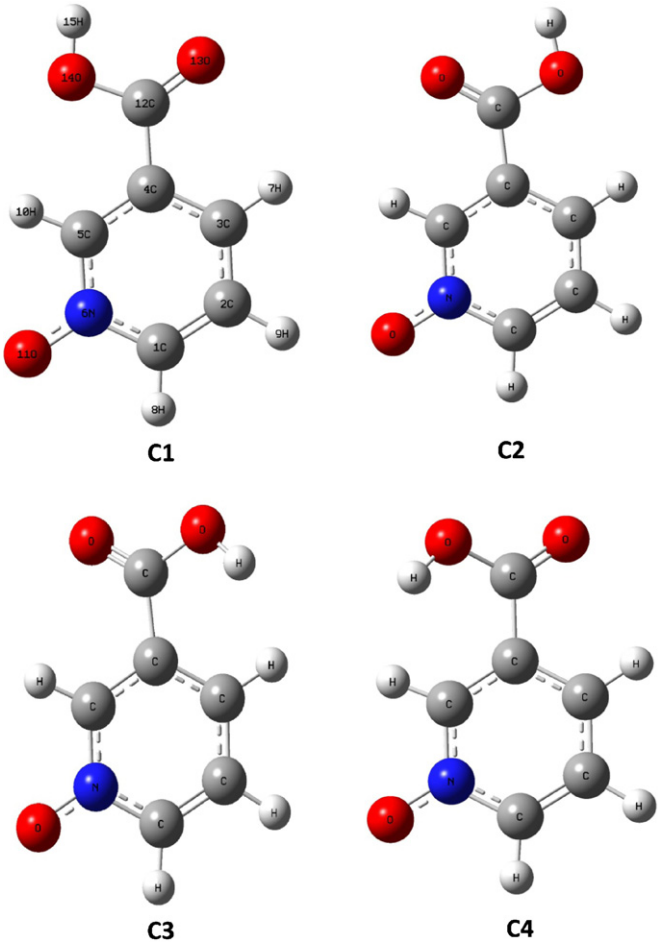

Fig. 1. The theoretical geometric structures of NANO.

After optimization, ^{1}H and ^{13}C NMR chemical shifts (δ_H and δ_C) were calculated using the GIAO method [36] in DMSO. CIS method is proved to be a powerful and effective computational tool for study of ground and excited state properties by comparison to the available experimental data. Hence, we used CIS method to obtain wavelengths λ_{max} and compare with the experimental UV absorption of NANO.

4. Results and discussion

There are four possible conformers for NANO molecule, illustrated in Fig. 1, dependent on the positions of the hydrogen atoms bonded to oxygen, whether they are directed away from or toward the ring. Four conformers of NANO molecule energies and energy difference [the relative energy of the other conformers was as: $\Delta E = E(C_n) - E(C1)$, the conformer C1 is the lowest energy as reference point] are determined in Table 1. Our calculations show that the four conformations for title molecule, do not differ greatly in energy, but demonstrate that conformation C1 and C2 have the lowest energy. From the DFT calculation of conformers with 6-311++G(d,p) basis set, the conformer C1 is predicted more stable from 0.2835 kcal/mol to 7.6621 kcal/mol than the other conformers. Additionally, because of the imaginary frequency, the calculations showed the conformers C3 and C4 to be unstable conformer. Intra-hydrogen bonds can be responsible for the geometry

Table 1
Calculated energies and energy differences for four conformers of NANO.

Conformers	Energy		Energy differences[a]	
	Hartree	kcal/mol	Hartree	kcal/mol
C1	−512.17299495	−321393.4200	0.0000	0.0000
C2	−512.17254311	−321393.1364	0.0005	0.2835
C3	−512.16121957	−321386.0308	0.0118	7.3892
C4	−512.16078462	−321385.7579	0.0122	7.6621

[a] Energies of the other three conformers relative to the most stable C1 conformer.

and the stability of a predominant conformation; the formation of hydrogen bonding between a hydroxyl and O=COH cause the structure of the conformer C1 to be most stable conformer. Therefore, the discussion below refers only to this C1 conformer.

The most stable structure, which has C_s symmetry group, consists of 15 atoms, so it has 39 fundamental vibrational modes. These modes are represented by symmetry species 27A′ + 12A″, with A′ representing in-plane motions and A″ representing out-of-plane motions. We reported some geometric parameters (bond lengths and bond angles), vibrational frequencies, NMR shifts and UV absorption for title molecule by using B3LYP 6-311++G(d,p) by comparing experimental results.

4.1. Geometrical structures

X-ray diffraction of the nicotinic acid molecule was studied [37]. Since the crystal structure of NANO and its dimer structure are not available in the literature till now, the geometric parameters, bond lengths and bond angles, compared with the nicotinic acid. The atomic numbering schemes of all conformers (C1, C2, C3, and C4) of NANO are shown in Fig. 1. Also, the dimer of C1 conformer is shown in Fig. 2. The calculated bond lengths and bond angles for NANO and its dimer conformer are tabulated in Table 2 in comparison to the experimental values.

The C–C and C=C bond lengths in the ring are measured at 1.378, 1.379, 1.385 and 1.388 Å for nicotinic acid [37]. The optimized C–C bond lengths in NANO fall in the range 1.381–1.397 Å. These values show that our calculation results are more consistent with the experimental data. Calculated C–N bond length is shorter than 0.3 Å observed value. C_{ring}–C_{COOH} bond length was calculated 1.492 Å and it shows good agreement with the experimental data of 1.482 Å. In international tables for crystallography [38] the CO bond lengths in the carboxylic acid group conform to the average values are tabulated for an aromatic carboxylic acid in which C=O is 1.226 (20) Å and C–O is 1.305 (20) Å. For nicotinic acid, the C–O bond lengths in carboxyl group in which C=O is 1.184 Å and C–O is 1.338 Å [37]. In this study, we calculated 1.2062 Å (C=O) and 1.352 Å (C–O) for NANO.

The C1–C2–C3, C2–C3–C4, C3–C4–C5, C1–N6–C5, C4–C5–N6 and C2–C1–N6 bond angles are observed 119.2°, 119.1°, 117.8°, 117.5°, 124.0° and 122.4°, which calculated 120.6°, 117.8°, 120.4°, 118.6°, 121.2° and 121.4°, respectively. Due to addition of O atom

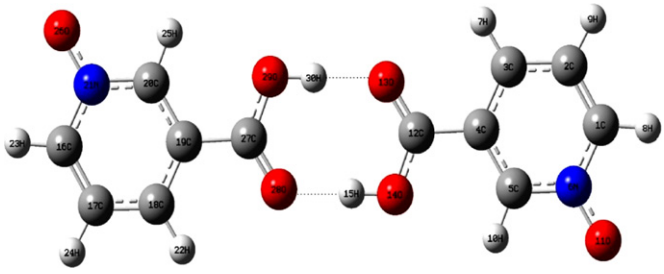

Fig. 2. C1 dimer conformer of NANO.

Table 2
Comparison of geometric parameters, bond lengths (Å), and bond angles (°), for the monomer and dimer C1 conformer of NANO calculated by the B3LYP 6-311++G(d,p) method.

Parameters	Exp. X-ray[a]	Theoretical	
		Monomer	Dimer
Bond lengths (Å)			
C1–C2	1.385	1.381	1.381
C1–N6	1.343	1.373	1.374
C1–H8		1.080	1.080
C2–C3	1.378	1.391	1.391
C2–H9		1.083	1.083
C3–C4	1.388	1.397	1.397
C3–H7		1.081	1.081
C4–C5	1.379	1.387	1.387
C4–C12	1.482	1.492	1.491
C5–N6	1.336	1.369	1.369
C5–H10		1.079	1.079
N6–O11		1.276	1.275
C12–O13	1.184	1.206	1.227
C12–O14	1.338	1.352	1.319
C14–H15		0.969	0.999
H15···O28			1.668
O13···H30			1.668
Bond Angles (°)			
C2–C1–N6	122.4	121.4	121.4
C2–C1–H8		124.9	124.9
N6–C1–H8		113.7	113.7
C1–C2–C3	119.2	120.6	120.6
C1–C2–H9		118.4	118.4
C3–C2–H9		121.0	121.0
C2–C3–C4	119.1	117.8	117.8
C2–C3–H7		122.3	122.3
C4–C3–H7		119.9	120.0
C3–C4–C5	117.8	120.4	120.5
C3–C4–C12	118.2	118.8	119.4
C5–C4–C12	124	120.8	120.1
C4–C5–N6	124	121.2	121.2
C4–C5–H10		124.4	124.3
N6–C5–H10		114.4	114.6
C1–N6–C5	117.5	118.6	118.6
C1–N6–O11		120.7	120.7
C5–N6–O11		120.7	120.7
C4–C12–O13	124	124.3	121.6
C4–C12–O14	114.1	112.8	114.3
O13–C12–O14	121.9	122.9	124.1
C12–O14–H15		107.3	110.4
C12–O13···H30			127.0
H15···O28–C27			127.0

[a] Taken from ref. [37].

at the N6 site in nicotinic acid some bond angles are slightly larger than each other (see Table 2). Intermolecular hydrogen bonds for dimeric structure are almost linear (the O–H···O angle equals 177.0°) and O···O bond lengths 2.674 Å [39]. Similarly, we calculated this angles and lengths 178.5° and 2.66 Å. The small difference between the computed values is due to the reason that calculation belongs to gaseous phase and experimental result belongs to solid phase.

4.2. NMR spectra

Experimental and theoretical chemical shifts of NANO are recorded and calculated. The experimental ^{1}H and ^{13}C NMR spectra (in DMSO solution) of NANO are shown in Fig. 3a and b. Full geometry optimization of NANO was performed at the gradient corrected DFT using the hybrid B3LYP method based on Becke's three parameters functional of DFT. Then, gauge-including atomic orbital (GIAO) ^{1}H and ^{13}C NMR chemical shift calculations of the compound has been made by same method using 6-311++G(d,p) basis set with IEFPCM model in DMSO solution. Application of the GIAO [40] approach to molecular systems was significantly

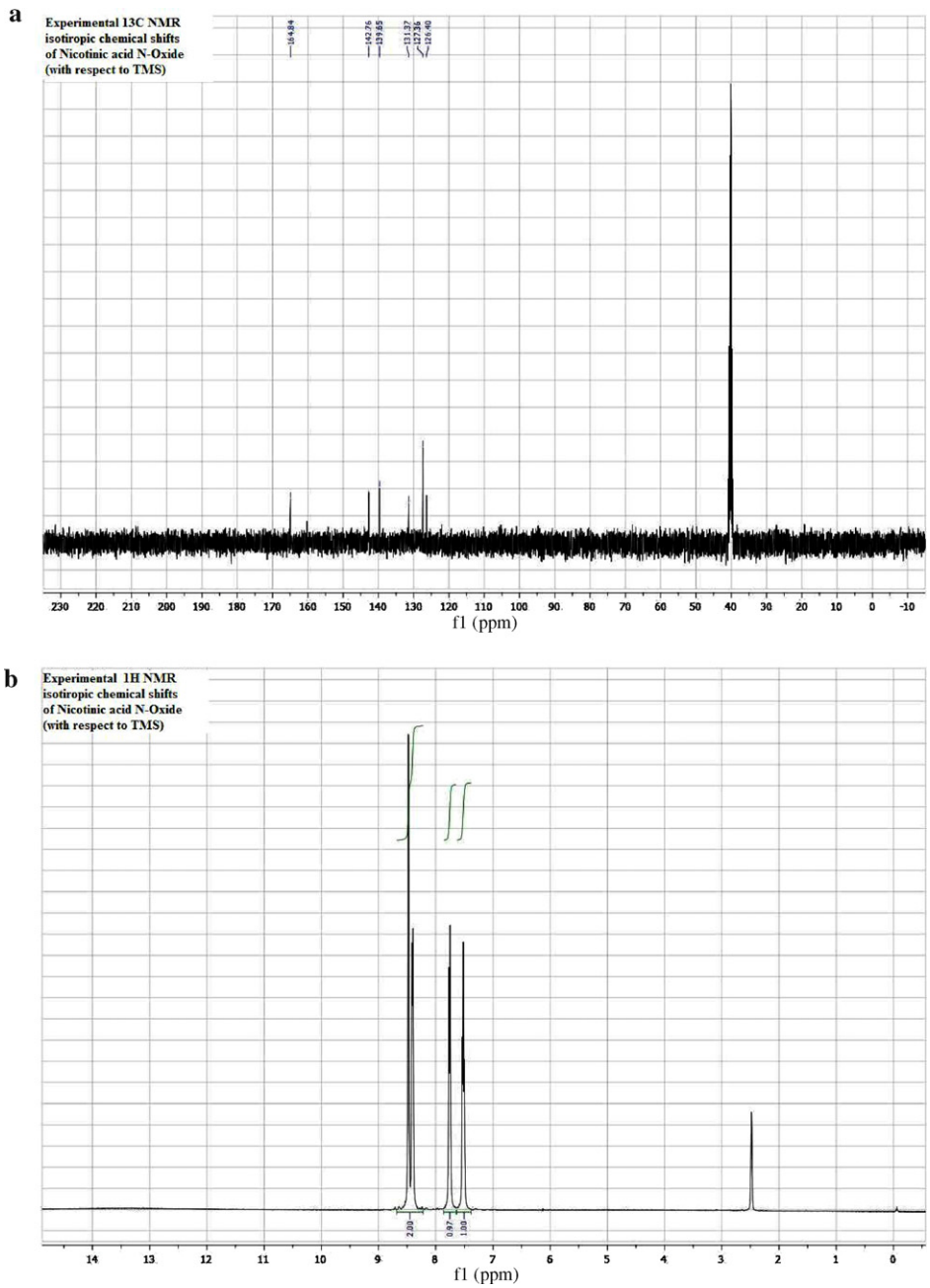

Fig. 3. The experimental (a) ^{13}C NMR spectrum and (b) ^{1}H NMR spectrum of NANO in DMSO.

improved by an efficient application of the method to the ab-initio SCF calculation, using techniques borrowed from analytic derivative methodologies. Relative chemical shifts were estimated by using the corresponding TMS shielding calculated in advance at the same theoretical level as the reference. The obtained data, compared with experimental data, are gathered in Table 3. Atom positions were numbered according to the Fig. 1.

As can be seen from the Table 3, ^{1}H NMR isotropic chemical shifts were calculated at 8.86, 8.43, 7.98, 7.56 and 6.63 ppm, observed at 8.47, 8.41, 7.77 and 7.54 ppm. The H_{15} atom is not observed any chemical shift NMR spectrum due to the DMSO solution. Chemical shift of proton numbered H_{10} is higher than that of the H_8 atom. It means that the electronic charge density around the H_8 is lower than H_{10} and C1=C2 bond decrease chemical shift at the ring proton of H_8.

Table 3
Experimental and calculated ^{1}H and ^{13}C NMR chemical shifts (ppm) of NANO.

Atom position	Experimental	Theoretical
C12	164.84	168.08
C1	142.76	149.45
C5	139.65	148.05
C4	131.37	132.50
C2	127.36	129.47
C3	126.40	126.95
H10	8.47	8.86
H8	8.41	8.43
H7	7.77	7.98
H9	7.54	7.56
H15		6.63

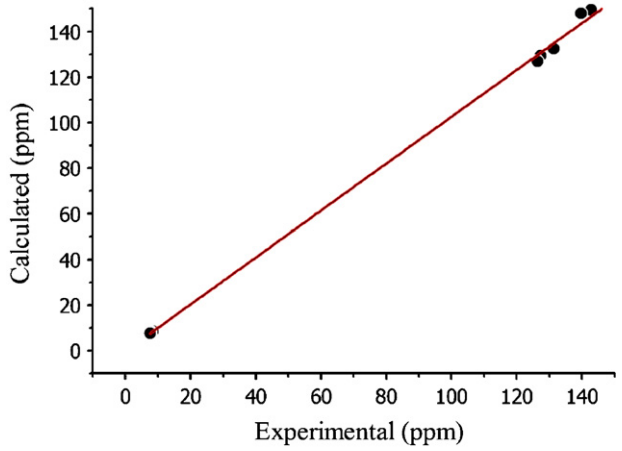

Fig. 4. Correlation graphic of calculated and experimental chemical shifts of NANO.

NANO molecule has six different carbon atoms, therefore six chemical shifts are observed in ^{13}C NMR spectrum. Taking into account that the range of ^{13}C NMR chemical shifts for a typical organic molecule usually occur >100 ppm [41,42] the accuracy ensures reliable of spectroscopic parameters. In the present paper, ^{13}C NMR chemical shifts in the ring for the title compound are >100 ppm, as expected (Table 3). The signal of aromatic carbon atoms was observed at 142.76, 139.65, 131.37, 127.36 and 126.40 ppm which was calculated at 149.45, 148.05, 132.50, 129.47, 126.95 ppm. All computations are in good agreement with experimental data. The carboxyl group which is an electronegative functional group polarizes the electron distribution, therefore the calculated^{13}C NMR chemical shift value of C12 bonded to carboxyl group is too high, observed at 164.84 ppm while which was calculated at 168.08 ppm. Similarly, C1 and C5 atoms have larger ^{13}C NMR chemical shifts than the other ring carbon atoms. DMSO contains electronegative atoms such as oxygen and sulfur. Thus in our title molecule was affected this solution.

The relations between the calculated and experimental chemical shifts (δ_{exp}) are usually linear and described by the following equation:

$$\delta_{cal}\ (\text{ppm}) = 1.0282\delta_{exp} - 0.1649 \quad (R^2 = 0.9989)$$

Also, in present study, the following linear relationships were obtained for ^{1}H and ^{13}C chemical shifts.

$$^{1}\text{H} : \delta_{cal}\ (\text{ppm}) = 1.1608\delta_{exp} - 1.1336$$

$$^{13}\text{C} : \delta_{cal}\ (\text{ppm}) = 1.0775\delta_{exp} - 7.0700$$

The performance of the B3LYP method was quite close for chemical shifts. However, ^{13}C NMR calculations gave a slightly better coefficient and lower standard error (R^2 = 0.9646) than for ^{1}H (R^2 = 0.9176) chemical shifts. Based on the ^{1}H and ^{13}C NMR chemical shifts data collected in Table 3 one can deduce that qualitatively the ^{13}C and ^{1}H NMR chemical shifts of NANO are described fairly well by the selected DFT method combined with the basis set. The correlations between the experimental and calculated chemical shifts obtained by DFT/B3LYP method are given in Fig. 4.

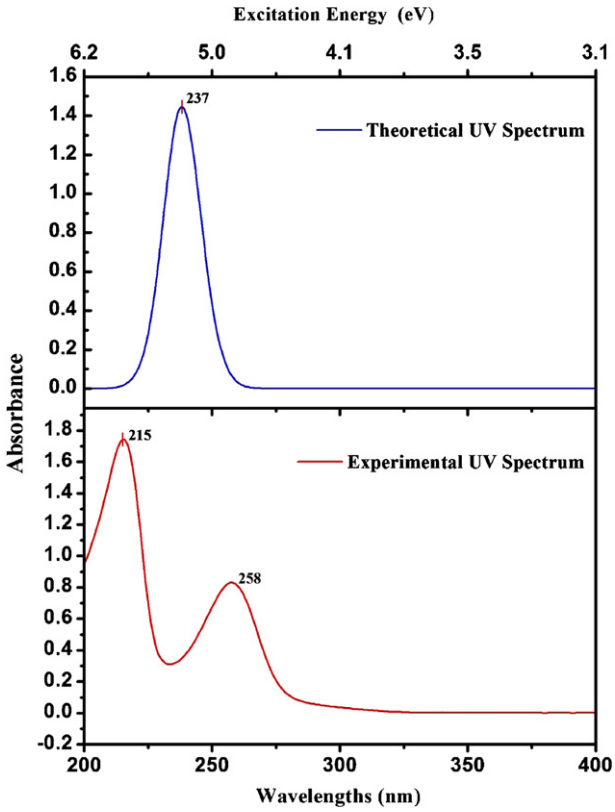

Fig. 5. The experimental UV spectrum of NANO in water.

4.3. UV spectrum and electronic properties

The UV spectrum of NANO, shown Fig. 5, was measured in water solution. The experimental absorption wavelengths (energies) and computed electronic values, such as absorption wavelengths (λ), excitation energies (*E*), oscillator strengths (*f*), major contributions of the transitions and assignments of electronic transitions are tabulated in Table 4. The absorption wavelengths are observed at 258 nm and 215 nm and calculated at 237 nm and 226 nm. GaussSum 2.2 program [43] was used to calculate group contributions to the molecular orbitals (HOMO and LUMO) and prepare the density of states (DOS) spectra in Fig. 6a and b. The DOS spectra were created by convoluting the molecular orbital information with GAUSSIAN curves of unit height. The calculations of the electronic structure of NANO were optimized in singlet state. Then, the electronic transition was calculated by using CIS/6-311++G(d,p) method. Both the highest occupied molecular orbital (HOMO) and lowest unoccupied molecular orbital (LUMO) are the main orbital taking part in chemical reaction. The HOMO energy characterizes the ability of electron giving whereas LUMO energy characterizes the ability of electron accepting, and the gap between HOMO and LUMO characterizes the molecular chemical stability. The energy gap between the HOMO and the LUMO, is a critical parameter in determining molecular electrical transport properties because it is a measure of electron conductivity [44]. According to Fig. 6a, the HOMO of steady compound presents a charge density that did

Table 4
Experimental and calculated wavelengths λ (nm), excitation energies (*E*), oscillator strengths (*f*) in water solution.

Experimental		Calculated			Assignments	Major contributes
λ (nm)	*E* (eV)	λ (nm)	*E* (eV)	*f*		
258	4.81177	237	5.20986	0.1973	π–π*	H → L+1 (73%)
215	5.77412	226	5.48578	0.0099	π–π*	H → L+4 (54%), H−1 → L+1 (27%)

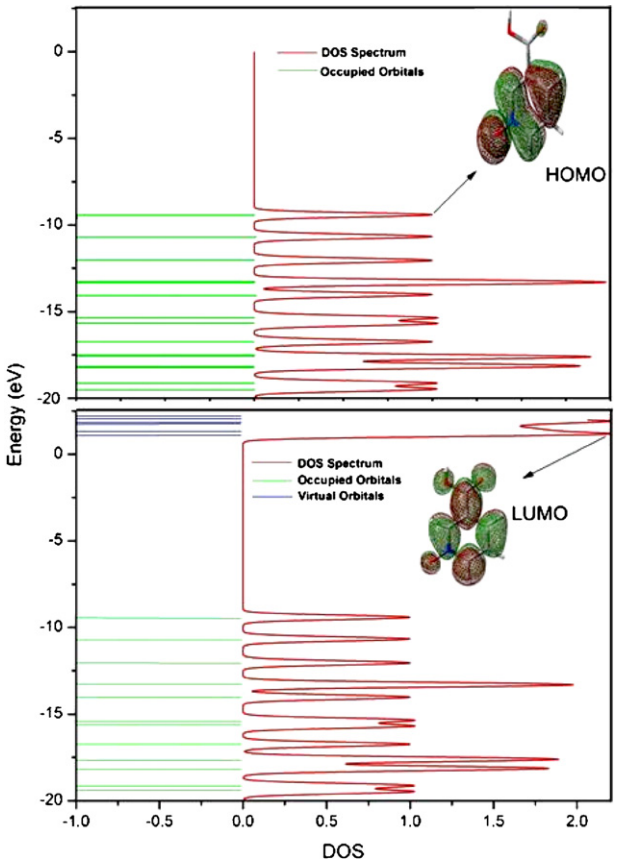

Fig. 6. Density of states (DOS) diagrams for NANO.

not localize only on the COH group and H9 atom while the LUMO (Fig. 6b) is characterized by a charge distribution of all atoms in our molecule. The experimental band at 258 nm is attributed mainly to HOMO → LUMO+1 transition with 73% contribution. This transition is predicted as π–π^* transition. The other wavelength, assignments and calculated counterparts with major contributions can be seen in Table 4. The energy value of HOMO is computed at −9.4 eV and LUMO is 1.13 V, and the energy difference is 10.53 eV in water for title molecule. The results are illustrated in Fig. 7. Moreover lower in the HOMO and LUMO energy gap explains the eventual charge transfer interactions taking place within the molecule.

4.4. Vibrational spectral analysis

In order to obtain the spectroscopic signature of NANO molecule, we performed a wavenumber calculation analysis using DFT/B3LYP/6-311G++(d,p) basis set [30]. Calculations were made for free vacuum, whereas experiments were performed for solid samples; so there are some disagreements between calculated and observed vibrational wavenumbers.

Experimental and calculated Infrared and Raman spectra were presented in Fig. 8. The calculated IR and Raman spectra are shown in figure for comparative purpose, where the calculated intensity is plotted against harmonic vibrational wavenumbers. Experimental wavenumbers are tabulated in Table 5 together with the calculated wavenumbers for monomer and dimer C1 conformer of studied molecule individually. Modes are numbered from smallest to biggest wavenumber within each fundamental wavenumbers. The last column gives a detailed description of the normal modes based on the TED.

Due to the C=O stretching vibration, carboxylic group is observed a single band usually in the 1800–1700 cm^{-1} [26]. Koczon et al. [26] assigned C=O stretching vibration at 1708 cm^{-1} in IR and calculated at 1754 cm^{-1} for nicotinic acid. This band is assigned at 1721 cm^{-1} (FT-IR) and 1712 cm^{-1} (FT-Raman) for 2-Cl-nicotinic acid [9]. In solid state most of the carboxylic acids exist in dimeric

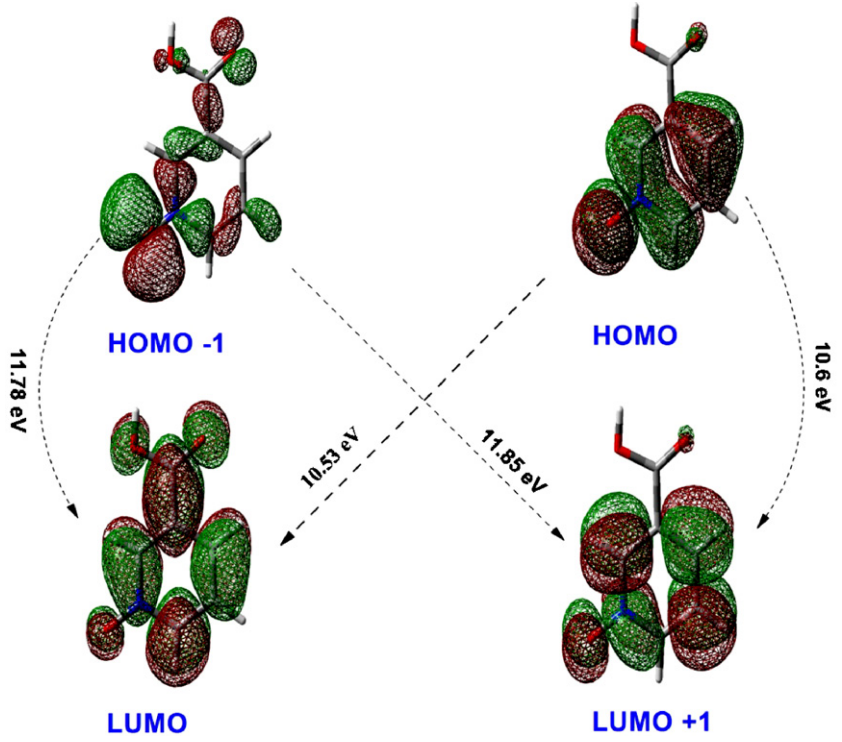

Fig. 7. The frontier and second frontier molecular orbitals of NANO.

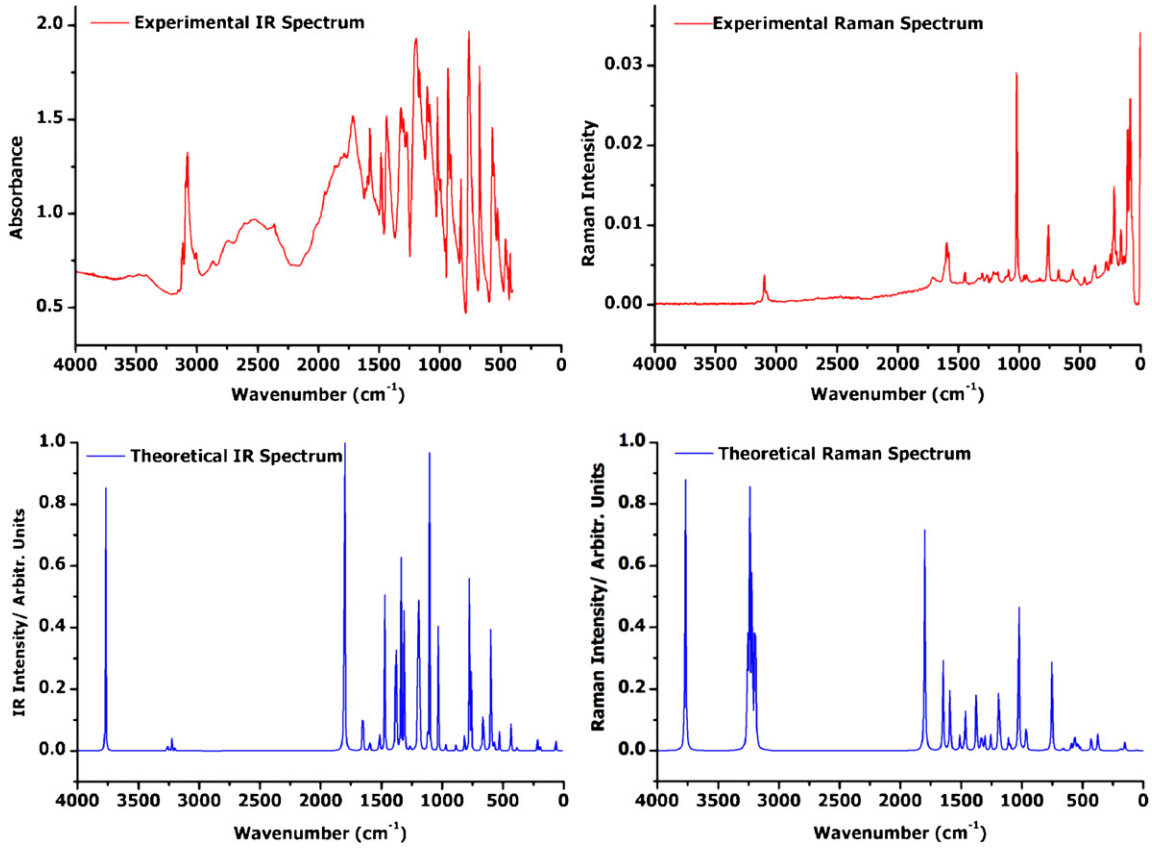

Fig. 8. Calculated and experimental Infrared and Raman spectrum of NANO.

form because of the inter-molecular hydrogen bonding between two –COOH groups. In such a case, two ν(C=O) are expected: one that is Raman active (symmetric stretching vibration) and the other one (anti-symmetric stretching vibration) is IR active only. Therefore, the C=O stretching mode ν_{34} is observed at 1622 cm^{-1} FT-IR spectrum and 1714 cm^{-1} in the FT-Raman spectrum. The theoretical value of C=O band is computed at 1723 cm^{-1}. However, the C=O stretching mode of dimer conformation was calculated 1669 and 1715 cm^{-1} which is in very good agreement with experimental data, because of the hydrogen-bonding effect the carboxyl groups. For dimer structure, the predicted value shows a small deviation of ca. 1 cm^{-1} at FT-Raman data.

Two other characteristic carboxylic group vibrations are: C–O stretching, ν(C–O) and C–O–H in-plane bending δ(C–OH) which are expected in the 1150–1450 cm^{-1} region depending on whether monomeric, dimeric or other hydrogen bonded species are present. The bands observed at 1086, 1211 and 1372 cm^{-1} assigned as C–O stretching and C–OH in-plane bending vibrations. These peaks are calculated at 1092, 1170 and 1351 cm^{-1} which exactly coincide with experimental values respectively. The C–COOH in-plane bending mode (ν_5) and (ν_3) are calculated at 367 cm^{-1} and 184 cm^{-1} and observed at 196 and 375 cm^{-1} in FT-Raman spectrum.

The free hydroxyl group absorbs strongly in the region 3700–3400 cm^{-1}. This may be combined effect of intermolecular hydrogen bonding. Koczon et al. [26] assigned OH stretching vibration at 3447 cm^{-1} IR and calculated at 3651 cm^{-1} for nicotinic acid. In this study, this band was recorded at 3684 cm^{-1} (FT-IR) and predicted at 3610 cm^{-1} which agreement with recorded FT-IR data. As expected this mode is pure stretching mode as it is evident from TED column, it is almost contributing 100%.

The OH in-plane bending occurs between 1440 and 1395 cm^{-1} and out-of-plane bending occurs between 960 and 875 cm^{-1} [45–47]. The O–H in-plane bending observed at 1372 cm^{-1} in FT-Raman while OH is assigned at 786 and 829 cm^{-1}, ν_{15} and ν_{16}, respectively. We calculated at 1351 cm^{-1} and 755, 796 cm^{-1}, in-plane bending and out-of-plane bending vibrations, respectively. For nicotinic acid, the OH in-plane bending is observed and calculated at 1370 and 1340 cm^{-1}, respectively [26]. The O–H in-plane bending and out-of-plane bending vibration values in dimer conformations are increasing, because of the hydrogen bonding effect through the carboxyl groups (see Table 5).

The hetero-aromatic structure shows the presence of the C–H stretching vibration in the 3000–3100 cm^{-1} range which is the characteristic region for ready identification of C–H stretching vibration [47]. In this region, the bands are not affected appreciably by the nature of the substituents. In aromatic compounds, C–H in-plane bending frequencies appear in the range of 1000–1300 cm^{-1} and C–H out-of-plane bending vibration in the range 750–1000 cm^{-1} [47,48]. For nicotinic acid, the C–H stretching modes are observed in the range 3104–3042 cm^{-1} and calculated in the 3093–3046 cm^{-1} range [26]. In the present study, the four adjacent hydrogen atoms left around the ring the NANO give rise four C–H stretching modes (ν_{35}–ν_{38}), four C–H in-plane bending (ν_{23}, ν_{24}, ν_{25} and ν_{27}) and four C–H out-of-plane bending (ν_{16}, ν_{17}, ν_{18} and ν_{20}) vibrations which are corresponded to stretching modes of C1–H8, C2–H9, C3–H7 and C5–H10 units. These modes (ν_{35}–ν_{38}) are observed at 3022 and 3144 cm^{-1} in FT-IR (3080, 3098 and 3154 cm^{-1} in FT-Raman), predicted at 3062, 3087, 3104 and 3121 cm^{-1}. They are very pure modes since their TED contribution is 100%. The experimental magnitude of C–H stretching mode (ν_{38}) is larger than theoretical, due to attaching oxygen atom at the nitrogen atom in NANO molecule. The C–H in-plane bending vibrations (ν_{23}, ν_{24}, ν_{25} and ν_{27}) are observed at 1086, 1175, 1211 and 1300 cm^{-1}, calculated at 1092, 1161,

Table 5
Comparison of the calculated and experimental (FT-IR and FT-Raman) vibrational spectra for C1 conformers of NANO B3LYP/6311++G(d,p) basis set.

Modes	Sym.	Exp.		Theoretical monomer				Theoretical dimer		TED[b] (>10%)
No.	Species	FT-IR	FT-Raman	Unscaled freq.	Scaled freq.[a]	$I^{Infrared}$	I^{Raman}	Unscaled freq.	Scaled freq.[a]	
ν_1	A″			55	54	4.65	0.22	49–51	47–49	τCCC═O (51) + τCCC–O (46)
ν_2	A″		161	153	151	0.04	1.97	160–180	153–173	τCCCN (28) + τCCCC (22) + τCCCO (16) + τCCCH (18)
ν_3	A′		196	187	184	5.02	0.72	208–209	200–200	δCCC (65) + δC–COOH (22)
ν_4	A″		219	209	206	4.32	0.02	235–247	225–237	τCCNO (39) + τCCN (21) + τCHNO (14)
ν_5	A′		375	374	367	4.37	4.94	382–419	375–412	νC–COOH (33) + δCCC (17) + δO═C–O (13)
ν_6	A″	410		424	417	7.39	0.47	430–432	422–424	τCCCN (19) + τCCHN (18) + τCCH (17) + τCCCO (11)
ν_7	A′	430		430	422	7.70	3.44	435–438	425–429	δCCO (43) + δCNO (30)
ν_8	A″	478	462	520	511	9.02	0.79	439–465	431–457	τCCC (21) ring + τCCOH (19)) + τCCNO (13) + τCNCH (11)
ν_9	A′	532		540	531	0.23	2.44	537–539	528–530	δCNO (38) + δCCC (18) + δCCO (11) + δCNC (10)
ν_{10}	A′	560	558	564	554	9.58	5.81	544–549	535–540	δCCN (28) + δCCC (15) + δCNO (12) + δCCO (10) + δCCH (10)
ν_{11}	A″	594		591	581	93.64	1.77	569–580	560–570	τCCOH (38) + τCOOH (34)
ν_{12}	A′	686		654	643	43.95	0.55	666–666	655–655	δCOO (31) + δO–C═O (17) + δCCC (11)
ν_{13}	A″		676	670	658	6.11	0.36	681–690	669–678	τCCCN (33) + τCCCH (28) + τCNCH (16) + τCCCC (15)
ν_{14}	A′		759	753	740	20.94	22.74	764–767	751–754	νCC (19) + δCCC (11) trigonal ring breath + νCN (11)
ν_{15}	A″	786		768	755	91.11	0.49	775–788	762–775	τCCCO (33) + τCOOH (21) + τCCCH (17) + τCHNO (10)
ν_{16}	A″		829	810	796	4.53	0.24	808–810	794–796	τCCCH (19) + τCNCH (17) + τCCCO (17) + τCHN–O (13)
ν_{17}	A″	840		879	864	7.67	0.03	880–882	865–867	τCCCH (44) + τCHN–O (27) + τCNCH (12)
ν_{18}	A″	916		904	889	0.13	0.06	907–909	889–890	τCCCH (41) + τCHCH (26) + τCHN–O (12)
ν_{19}	A′	944	940	964	948	6.17	9.38	971–972	958–960	νCN (34) + νCC (13) + νON (10)
ν_{20}	A″	960	960	977	960	0.01	0.31	975–976	959–960	τCHCH (60) + τCCCH (14) + τCHCN (10)
ν_{21}	A′	998		1025	1008	44.30	39.19	1025–1026	1008–1008	νCC ring (23) + δCCC (20) tri ring breath + δCCN (18) + νCN (16)
ν_{22}	A′	1028		1098	1079	89.99	1.70	1105–1105	1086–1086	νCC ring (31) + νC–O (23) + δCCH (14) + δNCH (10)
ν_{23}	A′		1086	1111	1092	19.72	3.25	1133–1136	1114–1117	δCCH (34) + νCC (27) ring + νC–O (16)
ν_{24}	A′		1175	1181	1161	79.38	4.29	1183–1183	1163–1163	δCCH (48) + δCNH (18) + νCC (10) ring
ν_{25}	A′		1211	1190	1170	204.93	18.61	1256–1256	1234–1235	δCOH (34) + νCC (17) ring + νC–O (10) + δCCH (16)
ν_{26}	A′	1246		1255	1234	5.30	4.37	1283–1288	1261–1266	νCN (57) + νCC (31) ring
ν_{27}	A′	1300		1305	1283	81.22	4.00	1329–1332	1307–1309	νNO (28) + δCCH (28) + δCOH (12) + δCNH (10)
ν_{28}	A′		1304	1332	1309	87.02	6.34	1342–1344	1319–1321	δCCH (43) + νNO (25) + δCNH (13)
ν_{29}	A′		1372	1374	1351	189.08	17.32	1452–1464	1427–1439	δCOH (24) + νC–O (20) + νCC (17) + νNO (11)
ν_{30}	A′	1458	1445	1466	1441	77.11	12.52	1467–1482	1442–1457	νCC ring (28) + δCCH (19) ring + δNCH (19) ring
ν_{31}	A′	1502		1510	1485	25.50	5.05	1511–1511	1485–1486	νCC (33) ring + δCCH (28) + δNCH (11)
ν_{32}	A′	1584	1580	1591	1564	12.66	19.30	1591–1591	1564–1564	νCC (52) ring + δCCH (16) + νCN (14)
ν_{33}	A′	1604	1595	1647	1619	62.92	26.88	1646–1646	1618–1618	νCC (56) ring + δCNH (10)
ν_{34}	A′	1622	1714	1798	1723	363.80	77.09	1697–1744	1669–1715	νC═O (84)
ν_{35}	A′	3022		3196	3062	2.79	92.59	3119–3196	3066–3142	νCH (99)
ν_{36}	A′		3080	3222	3087	3.36	79.65	3196–3213	3142–3159	νCH (100)
ν_{37}	A′		3098	3241	3104	1.02	108.70	3225–3225	3170–3170	νCH (100)
ν_{38}	A′	3144	3154	3258	3121	7.43	51.97	3241–3241	3186–3186	νCH (100)
ν_{39}	A′	3684		3769	3610	114.73	138.64	3258–3258	3202–3202	νOH (100)

[a] Wavenumbers in the ranges from 4000 to 1700 cm^{-1} and lower than 1700 cm^{-1} are scaled with 0.958 and 0.983 for B3LYP/6-311++G(d,p) basis set, respectively [33].
[b] Total energy distribution: ν, stretching; δ, in-plane bending; τ; torsion.

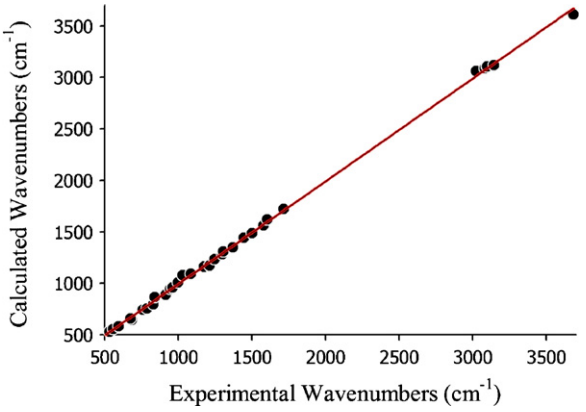

Fig. 9. Correlation graphic of calculated and experimental frequencies of NANO.

1170 and 1283 cm^{-1}, respectively. The C–H out-of-plane bending modes (ν_{16}, ν_{17}, ν_{18} and ν_{20}) are predicted at 796, 864, 889 and 960 cm^{-1}, observed at 829, 840, 916 and 960 cm^{-1}, respectively. Both the in-plane and out-of-plane bending vibrations are illustrated as mixed modes.

The ring stretching vibrations are much important in the spectrum of nicotinic acid and its derivatives are highly characteristic of the aromatic ring itself. The ring carbon–carbon stretching vibrations occur in the region 1430–1625 cm^{-1}. Koczon et al. [26] assigned CC stretching vibration at 1595, 1583, 1488 and 1449 cm^{-1} FT-IR and calculated at 1598, 1577, 1454 and 1414 cm^{-1} for nicotinic acid. In this study, the CC stretching modes are observed at 1458, 1502, 1584 cm^{-1} and 1604 cm^{-1}, calculated at 1441, 1485, 1564 and 1619 cm^{-1}.

The identification of CN vibrations is a very difficult task because of the mixing of several bands. Sundaraganesan et al. [49] assigned the band at 1689 cm^{-1} and 1302 cm^{-1} to C=N and C–N stretching vibration for benzimidazole, respectively. In this study, the C=N and C–N stretching vibrations are predicted at 1564 cm^{-1} and 1234 cm^{-1}, observed at 1246 cm^{-1} in FT-IR spectrum and 1580 cm^{-1} in FT-Raman spectrum (1584 cm^{-1} in FT-IR). These vibrations are also contaminated with C–C stretching and C–H bending vibrations as evident from last column of TED. These recorded bands ν_{26} and ν_{32} are in good agreement with the literature data [48]. The trigonal ring-breathing mode of the aromatic ring was observed at 759 and 998 cm^{-1} (ν_{14}, ν_{21}) in FT-IR spectrum, computed at 740 and 1008 cm^{-1} which are in very good agreement with the experimental results.

Non-planar deformation modes are (ν_4, ν_6, ν_8, ν_{13}, ν_{15}–ν_{18}) calculated 206, 417, 511, 658, 755, 796, 864 and 889 cm^{-1} and observed at 219, 410, 462 (478), 676, 786, 829, 840 and 916 cm^{-1} in FT-IR and FT-Raman spectrum.

The N–O vibration is predicted 455 cm^{-1} for nicotinamide *N*-oxide by Kumar et al. [50]. In this study, this band is observed at 430 cm^{-1} in FT-IR spectrum and calculated at 422 cm^{-1} that increases ca. 8 cm^{-1}.

We have drawn correlation graphics between the experimental and calculated wavenumbers that are obtained by DFT/B3LYP method (Fig. 9). The relations between the calculated and experimental wavenumbers are linear and are described by the following equation:

$$\upsilon_{cal} = 0.9981\upsilon_{exp} - 4.6497 \quad (R^2 = 0.9993)$$

We calculated RMS value between the calculated and experimental wavenumbers. As a result, the performances of the B3LYP method with respect to the prediction of the wavenumbers within the molecule were quite close.

Table 6
The bond distances (Å) and characteristic wavenumbers (cm^{-1}) related the C=O bond and O–H.

Conformers	C=O bond	Scaled wavenumbers	O–H bond	Scaled wavenumbers
	$D_{C12=O13}$	$\nu_{C12=O13}$	$D_{O14-H15}$	$\nu_{O14-H15}$
C1	1.206	1723	0.969	3610
C2	1.205	1723	0.969	3609
C3	1.198	1753	0.965	3647
C4	1.199	1751	0.965	3647

4.5. Bond distances and characteristic wavenumbers

The molecular structure of the most stable conformation has been widely investigated not only by experimental methods but also by theoretical approaches. Nicotinic acid and its derivatives establish one of the most popular model systems for studying inter- and intermolecular hydrogen bonds. In order to compare the strength of inter- and intermolecular hydrogen bonding, some pieces of evidence from geometrical and vibrational motion behavior were chosen to identify the hydrogen-bonding effect. Table 6 shows that the bond distances and the characteristic wavenumbers of atoms within various conformers or isomers. The relationships between these distances and the strengths of hydrogen bonds are discussed here. Based on these calculated values, we conclude the following:

(1) The carbonyl distance ($d_{C=O}$ bond length), which is the longest distance among the four conformers is C1, is calculated 1.206 Å and it has the smallest wavenumber ($\nu_{C=O}$) 1723 cm^{-1}. The previous work [51] we reported $d_{C=O}$ bond length as 1.225 Å for the C1 conformer (which is longer than the other eight conformers) for of the 5-fluoro- and 5-chloro-salicylic acid. Similar results were obtained for different molecules [10,52,53].
(2) Due to the O atom attached in O=COH of the C1 and C2 conformer, which donates electron to form with H in hydroxyl only, they have the longest hydroxyl distances ($D_{O14-H15}$) (0.969 Å) and the smallest wavenumbers (ν_{O-H}) 3610 and 3609 cm^{-1}, respectively for NANO molecule. Similar results are obtained in the literature for different molecules [10,52,53].
(3) The calculated wavenumbers for dimer (intermolecular hydrogen bonding) NANO molecule shown in Fig. 2 are tabulated in Table 5. As seen in that table, the inter-hydrogen bonding effect through the carboxyl groups is clearly seen (e.g. in ν_{39}, ν_{34}, ν_{29}, ν_{25} modes). These results are in agreement with literatures [10,26,51–54].

5. Conclusion

In this paper, nicotinic acid *N*-oxide molecule was studied. Several properties were carried out using experimental techniques and tools derived from density functional theory. The optimized geometric parameters (bond lengths and bond angles) were theoretically determined at B3LYP/6-311++G(d,p) level of theory and compared with experimental (nicotinic acid) results. The vibrational FT-IR and FT-Raman spectra of nicotinic acid *N*-oxide were recorded. The magnetic properties of the title molecule were observed and calculated by B3LYP method using 6-311++G(d,p) basis set with IEFPCM model in DMSO solution. The chemical shifts were compared with experimental data, showing a very good agreement both for ^{13}C and ^{1}H. Due to the DMSO solution one chemical shift was not observed for ^{1}H NMR in the carboxyl group. The electronic properties were also calculated and experimental electronic spectrum was recorded with help of UV–vis spectrometer. The maxima absorption wavelengths were observed 215 and

258 nm which are possibly due to the $\pi \rightarrow \pi^*$ transition. The comparison of predicted bands with experimental was done and shows an acceptable general agreement. From the results, the carbonyl distance (C=O) is longer, its wavenumber is smaller.

Acknowledgement

This work was supported by the Celal Bayar University Research fund through research Grant No: FBE-2008/54.

References

[1] R. Altschul, A. Hoffer, J.D. Stephen, Arch. Biochem. Biophys. 54 (1955) 558–559.
[2] S. Everts, Chem. Eng. News 86 (2008) 15–23.
[3] C.L. Broadhurst, W.F. Schmidt, J.B. Reeves, M.M. Polansky, K. Gautschi, et al., J. Inorg. Biochem. 66 (1997) 119–130.
[4] N.K. Singh, D.K. Singh, et al., Synth. React. Inorg. Met.-Org. Chem. 32 (2002) 203–218.
[5] J.S. Loring, M. Karlsson, W.R. Fawcett, W.H. Casey, Geochim. Cosmochim. Acta 64 (2000) 4115–4129.
[6] F. Bardak, A. Ataç, M. Kurt, Spectrochim. Acta 71 (2009) 1896–1900.
[7] N. Can, A. Ataç, F. Bardak, Ş.E.S. Can, Turk. J. Chem. 29 (2005) 589–595.
[8] A. Ataç, F. Bardak, Turk. J. Chem. 30 (2006) 609–618.
[9] M. Karabacak, M. Cinar, M. Kurt, J. Mol. Struct. 885 (2008) 28–35.
[10] M. Karabacak, M. Kurt, Spectrochim. Acta A 71 (2008) 876–883.
[11] A. Albini, S. Pietra, Heterocyclic *N*-oxide, CRC Press, Boca Raton, USA, 1991.
[12] J. Balzarini, M. Stevens, E. De Clerc, D. Schols, C. Pannecouque, J. Antimicr. Chem. Chem. 16 (1977) 3314.
[13] N.A. Al-Masoudi, Y.A. Al-Soud, I.A. Al-Masoudi, Sulfur Lett. 24 (2000) 13–22.
[14] B.X. Li, R.L. Shang, B.W. Sun, Acta Crystallogr. E64 (2008) 131–137.
[15] S. Lis, Z. Piskula, M. Kubicki, Mater. Chem. Phys. 114 (2009) 134–138.
[16] G.F. de Sa, O.L. Malta, C. de Mello Donega, A.M. Simas, R.L. Longo, P.A. Santa Cruz, E.F. da Silva Jr., Coord. Chem. Rev. 196 (2000) 165–195.
[17] S. Lis, Z. Piskula, M. Puchalska, J. Legendziewicz, J. Lumin. 221 (2007) 122–123.
[18] G. Meinrath, S. Lis, U. Bohme, J. Alloys Compd. 221 (2006) 408–412.
[19] N.S. Navaneetham, S. Soundarajan, Indian J. Chem. A (1981) 93–94.
[20] L. Yan, J.M. Liu, X. Wang, R.D. Yang, F.L. Song, Polyhedron 14 (1995) 3545–3548.
[21] M.A. Palafox, G. Tardajos, A.G. Martines, V.K. Rastogi, D. Mishra, S.P. Ojha, W. Kiefer, Chem. Phys. 340 (2007) 17–31.
[22] P.J. Stephens, F.J. Devlin, C.F. Chavalowski, M.J. Frisch, J. Phys. Chem. 98 (1994) 11623–11627.
[23] F.J. Devlin, J.W. Finley, P.J. Stephens, M.J. Frisch, J. Phys. Chem. 99 (1995) 16883–16902.
[24] S.Y. Lee, B.H. Boo, Bull. Korean Chem. Soc. 17 (1996) 754–759.
[25] S.Y. Lee, B.H. Boo, Bull. Korean Chem. Soc. 17 (1996) 760–764.
[26] P. Koczon, J.Cz. Dobrowolski, W. Lewandowski, A.P. Mazurek, J. Mol. Struct. 655 (2003) 89–95.
[27] M.R. Hudson, D.G. Allis, B.S. Hudson, Chem. Phys. Lett. 473 (2009) 81–87.
[28] W. Li-Ran, F. Yan, Chem. Phys. 323 (2006) 376–382.
[29] O. Sala, N.S. Gonçalves, L.K. Noda, J. Mol. Struct. 565–566 (2001) 411–416.
[30] M.J. Frisch, G.W. Trucks, H.B. Schlegel, G.E. Scuseria, M.A. Robb, J.R. Cheeseman, G. Scalmani, V. Barone, B. Mennucci, G.A. Petersson, H. Nakatsuji, M. Caricato, X. Li, H.P. Hratchian, A.F. Izmaylov, J. Bloino, G. Zheng, J.L. Sonnenberg, M. Hada, M. Ehara, K. Toyota, R. Fukuda, J. Hasegawa, M. Ishida, T. Nakajima, Y. Honda, O. Kitao, H. Nakai, T. Vreven, J.A. Montgomery Jr., J.E. Peralta, F. Ogliaro, M. Bearpark, J.J. Heyd, E. Brothers, K.N. Kudin, V.N. Staroverov, R. Kobayashi, J. Normand, K. Raghavachari, A. Rendell, J.C. Burant, S.S. Iyengar, J. Tomasi, M. Cossi, N. Rega, J.M. Millam, M. Klene, J.E. Knox, J.B. Cross, V. Bakken, C. Adamo, J. Jaramillo, R. Gomperts, R.E. Stratmann, O. Yazyev, A.J. Austin, R. Cammi, C. Pomelli, J.W. Ochterski, R.L. Martin, K. Morokuma, V.G. Zakrzewski, G.A. Voth, P. Salvador, J.J. Dannenberg, S. Dapprich, A.D. Daniels, O. Farkas, J.B. Foresman, J.V. Ortiz, J. Cioslowski, D.J. Fox, GAUSSIAN 09, Revision A.1, Gaussian Inc., Wallingford, CT, 2009.
[31] A.D. Becke, J. Chem. Phys. 98 (1993) 5648–5652.
[32] C. Lee, W. Yang, R.G. Parr, Phys. Rev. B37 (1988) 785–789.
[33] N. Sundaraganesan, S. Ilakiamani, H. Salem, P.M. Wojciechowski, D. Michalska, Spectrochim. Acta A 61 (2005) 2995–3001.
[34] J. Baker, A.A. Jarzecki, P. Pulay, J. Phys. Chem. A 102 (1998) 1412–1424.
[35] PQS Version 4.0, Beta, Parallel Quantum Solutions, Fayetteville, AR, USA, 2010.
[36] K. Wolonski, J.F. Hinton, P. Pulay, J. Am. Chem. Soc. 112 (1990) 8251–8260.
[37] W.B. Wright, G.S.D. King, Acta Crystallogr. 6 (1953) 305–317.
[38] F.H. Allen, Acta Crystallogr. B58 (2002) 380–388.
[39] A.R. Choudhury, T.N. Guru Row, Acta Crystallogr. E60 (2004) o1595–o1597.
[40] R. Ditchfield, Mol. Phys. 27 (4) (1974) 789–807.
[41] H.O. Kalinowski, S. Berger, S. Braun, Carbon-13 NMR Spectroscopy, John Wiley & Sons, Chichester, 1988, pp. 512–543.
[42] K. Pihlajer, E. Kleinpeter (Eds.), Carbon-13 Chemical Shifts in Structure and Spectrochemical Analysis, VCH Publishers, Deerfield Beach, 1994.
[43] N.M. O'Boyle, A.L. Tenderholt, K.M. Langer, J. Comput. Chem. 29 (2008) 839–845.
[44] K. Fukui, Science 218 (1982) 747–754.
[45] P. Venkoji, Indian J. Pure Appl. Phys. 24 (1986) 166–172.
[46] J. Marshal, Ind. J. Phys. 72B (1998) 661–667.
[47] M. Silverstein, G. Clayton Basseler, C. Morill, Spectrometric Identification of Organic Compounds, Wiley, New York, 2001.
[48] V. Arjunan, I. Saravanan, P. Ravindran, S. Mohan, Spectrochim. Acta A 74 (2009) 375–384.
[49] N. Sundaraganesan, S. Ilakiamani, P. Subramanian, B.D. Joshua, Spectrochim. Acta 67A (2007) 628–635.
[50] M. Kumar, S. Jaiswal, R. Singh, G. Srivastav, P. Singh, T.N. Yadav, R.A. Yadav, Spectrochim. Acta A 74 (2010) 281–292.
[51] M. Karabacak, E. Kose, M. Kurt, J. Raman Spectrosc. 41 (2010) 1085–1097.
[52] Y. Akkaya, S. Akyuz, Vib. Spectrosc. 42 (2006) 292–301.
[53] M. Karabacak, M. Cinar, S. Ermec, M. Kurt, J. Raman Spectrosc. 41 (2010) 98–105.
[54] M. Karabacak, M. Kurt, J. Mol. Struct. 919 (2009) 215–222.